JOURNAL OF MATERIALS SCIENCE 31 (1996) 5077–5082

Investigations of metallic alloys for use as interconnects in solid oxide fuel cell stacks

S. LINDEROTH, P. V. HENDRIKSEN, M. MOGENSEN
Materials Department, Risø National Laboratory DK-4000 Roskilde, Denmark
N. LANGVAD
Haldor Topsøe A/S, DK-2800 Lyngby, Denmark

Some high-temperature alloys have been investigated in order to determine whether they are suitable as metallic interconnect materials in solid oxide fuel cell stacks. The requirements for such alloys are formulated. Thermal dilatometry and oxidation tests, as well as theoretical calculations of the stresses that are induced by differences in thermal expansion of the individual materials, have been performed. The results show that a chromium-rich alloy, with dispersions of fine Y_2O_3 particles, perform best among the samples investigated. Improvements are still needed in order to make the alloy fully applicable in a solid oxide fuel cell stack. Some suggestions for improvements are put forward.

1. Introduction

In the flat-plate design of solid oxide fuel cell (SOFC) stacks [1] the individual cells are interconnected by an electrical conductor which, at the same time, acts as a gas separator and distributor (fuel gas on the anode side of the cell and air on the cathode side). A sketch of a flat-plate SOFC stack is given in Fig. 1. The interconnect material is conventionally made of a ceramic material [1]. The technical requirements of the interconnect material strongly limit the number of useful ceramics. The ceramics normally used are $LaCrO_3$ doped with either CaO or SrO [1].

There are several reasons [2, 3] why the interconnect material preferably should be made of a metallic alloy:

(i) material costs: lanthanum is an expensive rare-earth element; typical transition elements of high-temperature alloys (nickel, iron, cobalt, chromium) are substantially cheaper;

(ii) mechanical properties: strength and workability of metals is, in general, much better for metals than for ceramics;

(iii) electrical conductivity of metals is about three orders of magnitude higher than for doped $LaCrO_3$;

(iv) the heat conductivity of metals is typically much higher than for doped $LaCrO_3$. Improved heat conductivity will reduce stresses that occur due to temperature gradients in the fuel cell stack and reduce the demand for cooling by excess gas.

Hence, a search for potential metallic alloys has been started [4–6]. Some of the requirements for a metal to be used as an interconnect material are:

1. the thermal expansion coefficient (TEC) must be close to that of the other cell elements, and particularly, it must be close to that of the electrolyte (YSZ = yttria stabilized zirconia), i.e. around $11 \times 10^{-6}\,K^{-1}$ in the temperature interval between the temperature of assembly and room temperature;

2. the metal must show good resistance against high-temperature corrosion (e.g. oxidation, carburization and nitridation);

3. the oxide layer formed on the metal surface must have a good adhesion to the metal and the electrical resistivity of both the oxide layer and the interface between metal and metal oxide must be low;

4. reactions of alloy and oxide layer with the electrodes must not diminish the cell properties. Among unwanted reactions is evaporation of oxide, e.g. CrO_3 on to the catalytic active surfaces of the electrodes;

5. the metal must be gas tight and the permeability of H^+ and O^{2-} must be low;

6. the price of the alloy in the final form must be sufficiently low to make the SOFC technology commercially feasible.

We consider requirements 1 and 2 in the above list to be the criteria best suited for determination of whether an alloy is interesting for use as a metallic interconnect. In designs where the cells and the interconnect are bonded together, TEC matching is essential in order to avoid detrimental residual stresses building up upon cooling. In this work, we have therefore been focusing on experimental studies of the thermal expansion of the alloys and their high-temperature corrosion behaviour as well as theoretical estimates of induced thermal stresses in the stack components due to mismatch in thermal expansion coefficients. Estimates of the electrical resistances of the oxide scales have also been made.

0022–2461

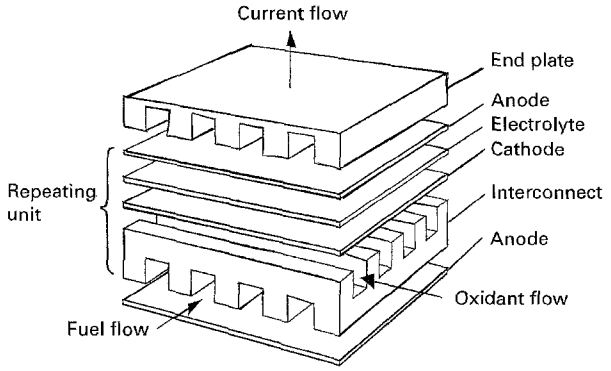

Figure 1 Sketch of the flat-plate design of a solid oxide fuel cell (SOFC) stack.

TABLE I Selected alloys and their nominal compositions deduced from the suppliers' data sheets

Name	Supplier	Composition*				
		Ni	Fe	Cr	Al	Other
Cr5Fe1Y_2O_3	Plansee	–	5	95	–	Y_2O_3
H-230	Haynes	57	3	22	0.3	14W, 2Mo
IN601	Inco	14	61	23	1.5	–
IN657	Cronite	48.5	–	48.5	–	1.5 Nb
APM	Kanthal	–	72	22	5.8	Ce

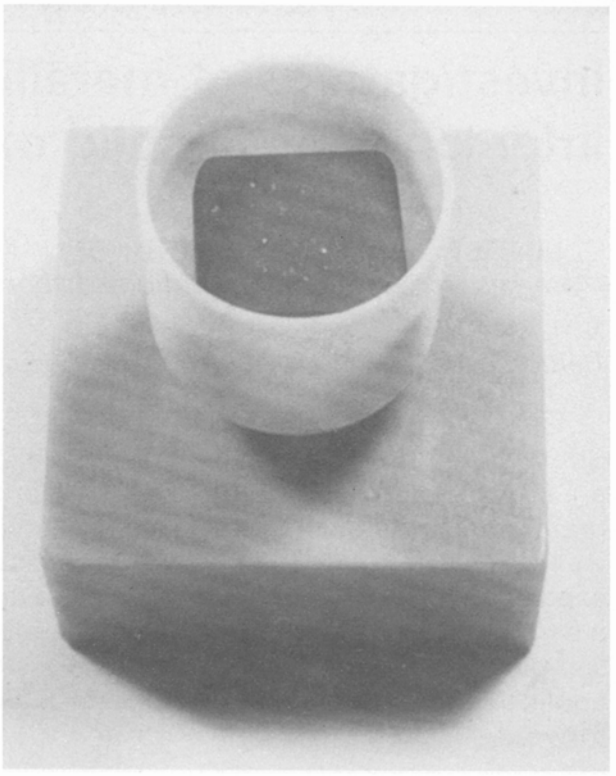

Figure 2 The figure shows the basket together with the $Cr_{94}Fe_5(Y_2O_3)_1$ sample from Metallwerk Plansee after thermogravimetric testing at 1000 °C for 100 h. Note the spots of oxide spallation of the alloy.

2. Experimental procedure

The alloys selected for investigation as potential metallic interconnect materials in SOFC stacks are given in Table I.

Thermogravimetric measurements at 1000 °C were made in a flow of dry air. The sample, with dimensions of about $11 \times 11 \times 4\ mm^3$, was placed in an alumina basket with an alumina top with holes to allow the gas to pass the sample. Fig. 2 shows the basket and sample after testing at 1000 °C. The samples were dry polished with 600-grit Al_2O_3 paper followed by cleaning in ethanol. The total exposure time was 100 h.

The structural characterization of the oxide scale after exposure to dry air at 1000 °C for 100 h was performed by using conventional X-ray diffraction (CuK_α radiation). The morphology of the scale surfaces, as well as cross-sections of selected samples, were studied by scanning electron microscopy (SEM).

Long-term isothermal oxidation studies were performed at 850 and 1000 °C in ambient air. The samples had sizes of about $14 \times 14 \times 4\ mm^3$. The treatments prior to testing were as for the samples prepared for thermogravimetric investigations. The samples were placed on top of four Al_2O_3 balls in an alumina container. The sample weight gains were measured after exposure times of 450 and 1800 h.

Microstructural characterizations of cross-sections of the 1800 h exposed samples were performed by optical microscopy and SEM.

Dilatometric investigations were performed on 20 mm long rods cut from bulk specimens. The length changes in the temperature range from room temperature to 1100 °C ($\Delta T = 5\ °C\ min^{-1}$) were compared to a simultaneously measured alumina sample. The measurements were performed by using a Setaram high-temperature dilatometer. The atmosphere was a flow of 3% H_2, 97% Ar in order to reduce effects of oxidation and nitridation. Two temperature cycles (RT–1100 °C–RT–1100 °C–RT) were made, the first cycle to allow for relaxation, while the second was used for the TEC determination.

3. Results and discussion

3.1. Oxidation resistance

The weight gain as a function of exposure time at 1000 °C in dry air is shown for the five examined samples in Fig. 3. The smallest weight gain is seen to be for the APM-Kanthal sample, while the two examined Inconel samples show the largest weight gain. The total weight gain after 100 h exposure is given in Table II.

The phases of the scales were determined by X-ray diffraction. The results are given in Table III. It should be noted that all but the APM-Kanthal sample form chromia as the external scale. The H-230 and Inconel 601 samples also form a spinel phase. The APM-Kanthal sample is an alumina-former but some haematite formation was also identified by X-ray diffraction.

Employing the fact that the Plansee alloy forms pure α-Cr_2O_3 as the external scale, and neglecting the minor oxide spallation and evaporation, the expected scale thickness can be calculated from the observed

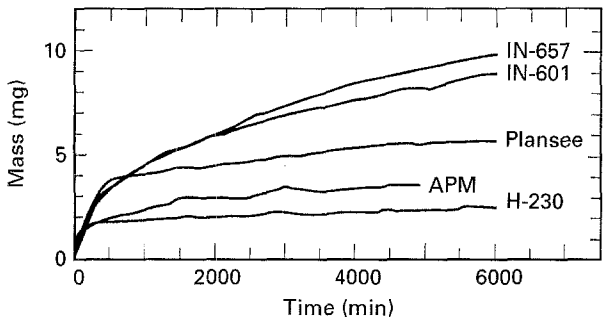

Figure 3 The weight gain for the examined samples at 1000 °C as a function of exposure time in dry air.

TABLE II Results of thermogravimetrical testing in dry air at 1000 °C for about 100 h. When the weight increase is assumed to be due to uptake of oxygen only, an increase of 1 mg cm^{-2} corresponds to an increase in scale thickness of 5 μm of Al_2O_3 or 6 μm Cr_2O_3, respectively.

Material	Δw (mg cm^{-2})
Plansee	1.3
H-230	0.9
IN601	2.1
IN657	2.3
APM	0.6

TABLE III The phases of the scales, after a 100 h testing in dry air at 1000 °C, as determined by X-ray diffraction

Plansee	α-Cr_2O_3
H-230	Cr_2O_3 + spinel
IN601	Cr_2O_3 + spinel
IN657	α-Cr_2O_3 + minor Cr_2N
APM	α-Al_2O_3 + α-Fe_2O_3

weight gain (see Table II) to be about 7.9 μm. An optical micrograph of the Plansee sample showed an average oxide layer thickness of about 8 μm, i.e. in good accordance with the thermogravimetric results.

Photographs of the samples tested at 1000 °C for 1800 h are shown in Fig. 4. The spallation of Haynes-230 and the Inconel samples is clearly visible. Oxide evaporation on to the walls of the container is seen in all cases except for APM-Kanthal.

Table IV gives the weight changes of the samples, with respect to their weights prior to oxidation, after 450 and 1800 h air exposure, respectively. The results given are for tests at both 850 and 1000 °C. The two Inconel-samples show significant oxide spallation at 850 °C. At 1000 °C, the Haynes-230 sample also shows significant spallation. Small-scale fractions of the Plansee samples were also seen to spall off. The APM-Kanthal sample showed the best resistance to oxide spallation. At 1000 °C, APM-Kanthal proved to have the best resistance against oxidation, while at 850 °C, the Haynes-230 sample had the best performance. The area specific weight gain for the 450 and 1800 h samples is generally seen to be larger than for the 100 h thermogravimetric testing (except for the Plansee alloy).

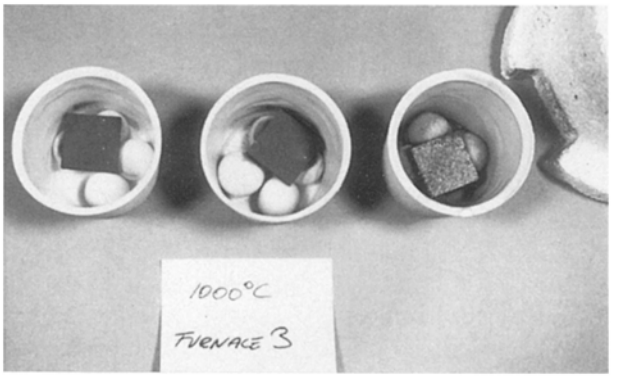

Figure 4 Photographs of three samples ($Cr_{94}Fe_5(Y_2O_3)_1$ (a) as-delivered, (b) polished and (c) H-230) in their respective containers after air-exposure for 1800 h at 1000 °C.

TABLE IV Weight changes of different after 450 and 1800 h air exposure at 850 and 1000 °C. (*) Severe oxide spallation occurred. The weight changes in these cases also include the weight of collected oxide that had spalled off

Sample	T (°C)	Δw (450 h) (mg cm^{-2})	Δw (1800 h) (mg cm^{-2})
Plansee as-received	850	0.57	0.63
Plansee		0.47	0.54
H-230		0.31	0.57
IN601		0.62	1.53*
IN657		0.76	0.75*
APM		0.54	0.81
Plansee as-received	1000	0.87	0.81
Plansee		0.95	1.04
H-230		1.22	1.80*
IN601		3.60	2.09*
IN657		1.14	5.75*
APM		0.68	0.68

Optical micrographs of cross-sections of the 1800 h tested samples are shown in Fig. 5. Significant internal oxidation of the Inconel 601 sample is seen to take place both at 850 and at 1000 °C. In accordance with the observed weight changes, the APM-Kanthal sample shows the thinnest and best adhering oxide layer. At 1000 °C only APM-Kanthal and the Plansee alloy do not show indications of internal oxidation. These two samples also show the thinnest oxide layer but significant buckling of the chromia scale on the Plansee alloy is observed after the 1000 °C testing.

3.2. Electronic resistivity

One of the important requirements for a metallic interconnect material is, as stated in Section 1, that the electrical resistivity across the protective oxide layer is kept at a reasonably low level. We estimate that the area specific electronic resistivity on each side of the metallic interconnect should not exceed about 25 mΩ cm^2 (which then in total would correspond to about half of the resistance [7] imposed by a 100 μm thick TZ8Y (cubic zirconia stabilized by 8 mol % yttria) electrolyte – the common electrolyte employed). Taking the oxide layer to be pure Cr_2O_3, the resistivity [8] due to 1 mg cm^2 oxide is approximately 60

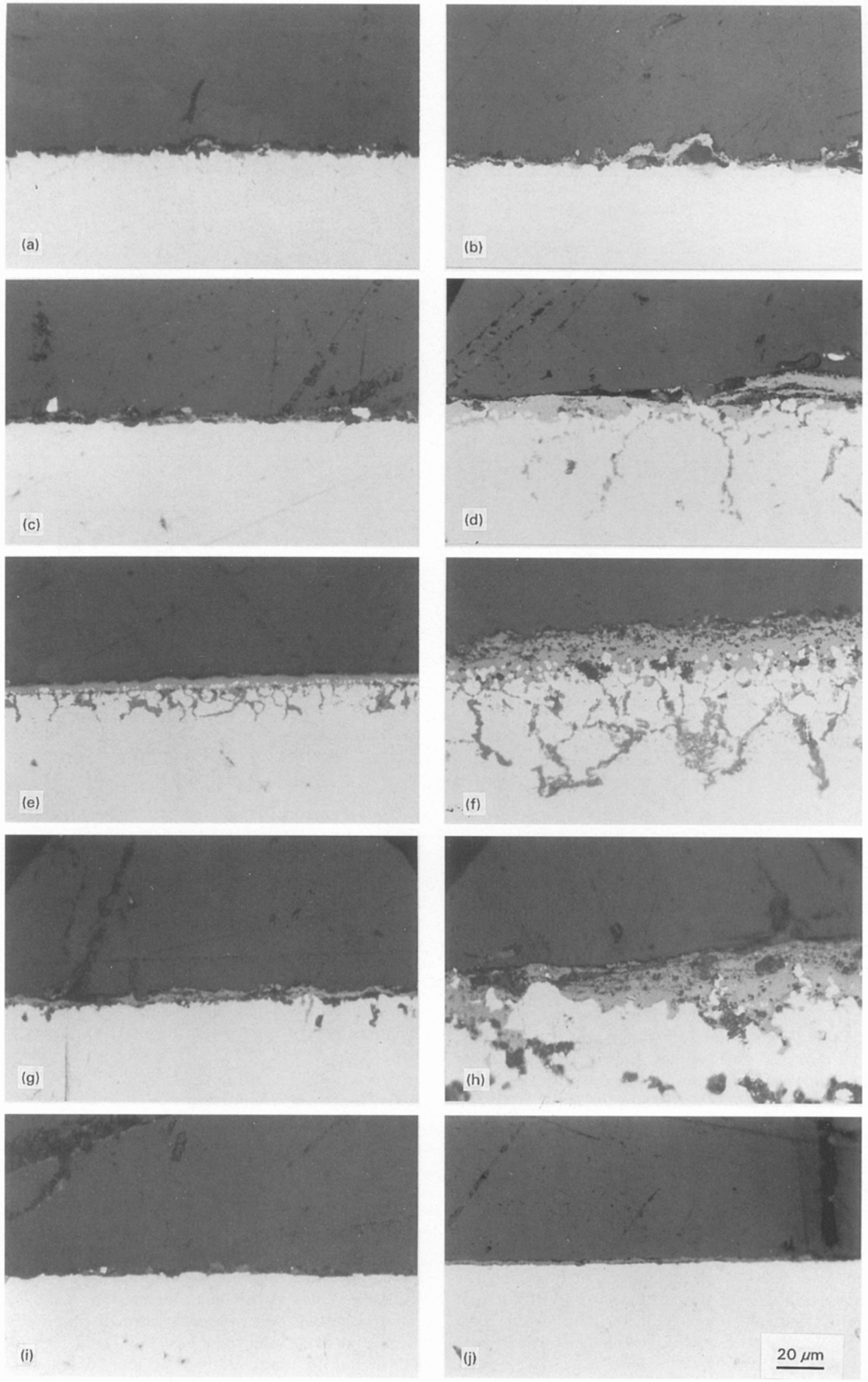

5080

TABLE V Results of dilatometric measurements. Analyses were carried out in the temperature interval 100–1000 °C in an argon atmosphere

Material	TEC (100–1000 °C) (10^{-6} K^{-1})
Plansee	11.8
H230	17.1
IN601	19.3
IN657	17.2
Kanthal-APM	16.3
YSZ-tape	10.9

and 20 mΩcm^2 at 850 and 1000 °C, respectively. Therefore, the resistivity of the metallic interconnect quickly, within a few hundred hours, becomes larger than the accepted upper value.

If the oxide instead consists of pure Al_2O_3, the area specific resistivity will be approximately a factor of 10^4 times larger than for pure Cr_2O_3, whence it is clear that from the point of view of electronic resistivity, a pure alumina former is not applicable as a metallic interconnect material. If an alumina former should be applied, the electrical conductivity of the oxide must be increased by, for example, doping. It must, though, be kept in mind that an increase of the electrical conductivity and a decrease of the oxidation rate are contradicting goals, hence a compromise must be sought.

3.3. Thermal expansion and thermally induced stresses

Another important requirement of an interconnect material is that the thermal expansion of the metal is close to that of the ceramic components [4, 9] (the electrolyte is considered to be the most critical component). Results of dilatometric measurements are summarized in Table V and the results are compared to the TEC of a typical electrolyte material (TZ8Y = cubic zirconia stabilized by 8 mol % yttria).

In order to help in estimating the acceptable TEC interval for a potential metallic interconnect material, the in-plane stresses of the individual components in a fuel cell stack when cooling from the stack sintering temperature have been calculated. It is assumed that the stack is in a stress-free state at the sintering temperature and that the symmetry of a cell stack will cause the stack to remain plane under stresses arising due to TEC mismatches (the latter has been confirmed by two-dimensional finite-element calculations). The individual layers will then be in either pure tension or in pure compression. The biaxial stress in the ith layer can [10], assuming temperature independent elastic constants, be written as

$$\sigma_i = E_i^*(\alpha - \alpha_i)\Delta T \quad (1)$$

Figure 5 Optical micrographs of cross-sections of the samples tested at (a, c, e, g, i) 850 °C and (b, d, f, h, j) 1000 °C for 1800 h in ambient air. (a, b) Plansee, (c, d) H-230, (e, f) IN601, (g, h) IN657 and (i, j) APM-Kanthal.

TABLE VI Values for E, ν and α for the different components of a solid oxide fuel cell. Materials parameters of the electrode materials are estimated values taking into account their large porosity (30–40 vol %)

Material	E (GPa)	ν	α (10^{-6} K^{-1})
Interconnect	280	0.29	–
YSZ-elektrolyte	200	0.30	10.8
Anode	65	0.25	12.8
Katode	65	0.25	12.0

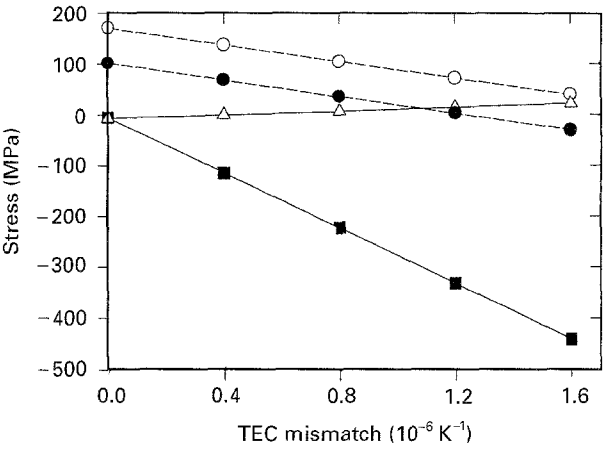

Figure 6 The in-plane stresses in the individual components as a function of the TEC difference between TZ8Y and a metallic interconnect material (ΔT = 1000 K). (- -○- -) Ni/YSZ cermet, (- - ●- -) LSM, (-△-) alloy, (-■-) YSZ.

where $E_i^* = E_i/(1 - \nu_i)$, E_i is Young's modulus, ν_i is Poisson's ratio, α_i is the thermal expansion coefficient of the ith layer, ΔT is the temperature difference between the sintering and the actual temperature, and

$$\alpha = \sum_1^N E_i h_i \alpha_i / E_i h_i \quad (2)$$

is the overall thermal expansion coefficient and N is the total number of layers in the multilayer.

In Table VI characteristic values for E, ν, and α are given for the different components of a solid oxide fuel cell. In Fig. 6 the calculated in-plane stresses of the individual components are shown as a function of the TEC difference between TZ8Y and a metallic interconnect material (assuming ΔT = 1000 K). It has been assumed that the TEC of the metal is larger than for the TZ8Y electrolyte, in which case it is clear that the electrolyte will be in compression. This is an advantage compared to ceramic interconnect materials where the electrolyte normally will be in tension (the strength of ceramics is typically substantially higher in compression than in tension). Owing to the relatively large TEC of the electrodes they will be in tension when the stack is cooled.

Only few experimental materials data are available, normally being room-temperature values. At elevated temperatures, Young's modulus especially can change significantly which will cause the built-up stresses in the components to alter. A proper determination of

allowable TEC values of the metallic interconnect should also include knowledge of mechanical strength values (e.g. fracture strength and toughness) of the components, particularly for the electrolyte.

The fracture strength of TZ8Y electrolyte tapes depends greatly on, for example, the preparation method of the tapes [11] ($\sigma = 350$ MPa, $m = 4.5$) and ($\sigma = 503$ MPa, $m = 10$), where σ and m are the average strength and the Weibull modulus, respectively, seem to represent the extremes of the reported [11, 12] experimental fracture strength values. If a probability of fracture of $p = 10^{-4}$ is assumed, acceptable TEC differences between the metallic interconnect and the TZ8Y electrolyte are approximately 0.2×10^{-6} and $0.8 \times 10^{-6}\,K^{-1}$ for the two cases, respectively. The employed values of fracture strength are obtained from three- or four-point bending tests, i.e. the tape strength values relate to tensional mode. The fracture strength of ceramics is much higher in compression than in tension (possibly by a factor of 15 [13], hence larger TEC mismatches can be tolerated.

If employing a different electrolyte, the above conditions would, off course, change. If, for example, TZ3Y (3 mol % yttria in zirconia; primarily tetragonal) is used instead of TZ8Y higher fracture strengths of the electrolyte tape can be obtained [14]. Fracture strengths (in tension) of TZ3Y may be larger than 1 GPa. At the same time, the toughness is better than for TZ8Y. When considering that the TEC of TZ3Y is $11.1\text{–}12.2 \times 10^{-6}\,K^{-1}$ between 100 and 1000 °C [15], i.e. closer to that of the high-temperature alloys, TEC differences of $3\text{–}6 \times 10^{-6}\,K^{-1}$ might be acceptable when using TZ3Y. The ionic conductivity of TZ3Y, however, is about a factor of three less than for TZ8Y at 1000 °C, a difference that becomes smaller at lower temperatures [16]. The lower conductivity may be compensated by using thinner electrolyte plates which, however, will affect the mechanical strength of the electrolyte.

4. Conclusion

The weight gain as a function of time of air exposure at 850 and 1000 °C of selected high-temperature alloys, have been measured. An alumina former (APM from Kanthal) showed the best resistance against oxidation, oxide spallation and oxide evaporation. Requirements of electrical conductivity through the oxide layer, however, makes pure alumina formers unattractive as interconnect materials. Modifications of the alumina (e.g. by doping) would be required. Tests of chromia-forming alloys have revealed that a chromium-rich alloy, with dispersions of Y_2O_3 particles, has the best performance regarding resistance against oxidation and spallation. However, some spallation and severe buckling of the oxide layer is observed even in this case. The oxidation rate of the chromium alloys is, although relatively low, sufficiently high to make the electrical resistance due to the oxide layer important even after only a few hundred hours at the operating temperature. The best alloys obtain an oxide layer thickness that for a pure chromia layer corresponds to an area specific electrical resistance of 60 and 20 $m\Omega\,cm^2$ at 850 and 1000 °C, respectively. The goal is to keep this contribution below about 25 $m\Omega\,cm^2$. Modifications of the chromia-forming alloys should preferably lead to lower oxidation rates and higher electrical conductivities of the oxide layer.

Besides good oxidation behaviour, a potential alloy for use as a metallic interconnect must not induce too large stresses in the ceramic component when the fuel cell stack is cooled down from the sintering temperature. Typical high-temperature alloys have thermal expansions that are substantially higher than for, for example, yttria-stabilized zirconia (TZ8Y). From a comparison of thermal expansion, calculated thermal stresses, and fracture strengths of TZ8Y, it follows that the $Cr_{94}Fe_5(Y_2O_3)_1$ alloy from Metallwerk Plansee, at present, seems to be the best candidate in this respect. Other electrolyte materials with higher fracture strengths and larger TEC values than TZ8Y are considered. TZ3Y is a possible electrolyte material which could increase the number of potential high-temperature alloys.

Future research on the implementation of metals as interconnect materials in solid oxide fuel cell stacks is suggested to focus on modifications of chromium-rich alloys in order to reduce the chromia formation rate and to improve on the electrical conductivity of the resulting oxide layer.

References

1. N. Q. MINH, *J. Am. Ceram. Soc.* **76** (1993) 563.
2. P. ZEGERS, in "Proceedings of the Third International Symposium on Solid Oxide Fuel Cells", edited by S. C. Singhal and H. Iwahara (The Electron Chemical Society, Pennington), Honolulu (1993) p. 16.
3. K. KRIST and J. D. WRIGHT, *ibid.* p. 782.
4. E. IVERS-TIFFÉE, W. WERSING, M. SCHIESSL and H. GREINER, *Ber Bunsenges. Phys. Chem.* **94** (1990) 978.
5. P. KOFSTAD and R. BREDESEN, *Solid State Ionics* **52** (1992) 69
6. T. KADOWAKI, T. SHIOMITSU, E. MATSUDA, H. NAKAGAWA, H. TSUNEIZUMI and T. MARUYAMA, *ibid.* **67** (1993) 65.
7. T. H. ETSEL and S. N. FLENGAS, *Chem. Rev.* **70** (1970) 339.
8. A. HOLT and P. KOFSTAD, *Solid State Ionics* **69** (1994) 137.
9. D. STOLTEN, E. MONREAL and W. MÜLLER, in "Proceedings of the Fuel Cell Seminar", edited by C. Pax *et al.* (Courtesy Associates, Washington), Tucson, AZ (1992).
10. O. T. IANCU and D. MUNZ, in "Joining of Ceramics, Glass and Metal", edited by W. Kraft (DGM, 1989) p. 257.
11. K. KENDALL, in "Proceedings of the Fuel Cell Seminar" edited by S. C. Singhal and H. Iwahara (The Electron Chemical Society, Pennington, Tucson AZ), (1992).
12. W. PRICE and K. KENDALL, in "Proceedings of the First European Solid Oxide Fuel Cell Forum", edited by U. Bossel, (1994) p. 757.
13. M. F. ASHBY, *Acta Metall.* **37** (1989) 1273.
14. S. P. S. BADWAL, *Solid State Ionics* **52** (1992) 23.
15. R. MÄNNER, E. IVERS-TIFFÉE and W. WERSING, in "Proceedings of the 2nd International Symposium on SOFC", edited by F. Grosz, P. Zegers, S. C. Singhal and O. Yamamoto (1991) p. 715.
16. F. T. CIACCHI, K. M. CRANE and S. P. S. BADWAL, *Solid State Ionics* **73** (1994) 49.

Received 3 October 1995
and accepted 24 April 1996